Nanowires

DOI: 10.1002/smll.200700753

Doping-Dependent Electrical Characteristics of SnO_2 Nanowires**

Qing Wan, Eric Dattoli, and Wei Lu**

Tin dioxide (SnO_2) represents an important metal-oxide group that can be suitable for a range of applications through the incorporation of dopants.[1] For example, the electrical conductivity of intrinsic SnO_2 depends strongly on the surface properties, as molecular adsorption/desorption will affect the band modulation and space-charge layer, which makes SnO_2 an important conductance-type gas-sensing material.[2,3] On the other end of the doping spectrum, degenerately donor (such as Sb, Ta, and F) doped SnO_2 films are important transparent conductive oxide (TCO) materials due to their large bandgap (3.6 eV) and high conductivity.[4,5] SnO_2-based TCO films are expected to be a low-cost alternative to indium tin oxide films in various optoelectronic devices, such as flat-panel displays, solar cells, and light-emitting diodes.

Recent studies have also found that transition metal (such as Co and Ni) doped SnO_2 acts as a diluted magnetic semiconductor and can exhibit Curie temperatures higher than room temperature.[6,7] On the other hand, extending the doping processes from bulk SnO_2 to nanostructures has been shown to be challenging due to both synthetic issues and ''self-purification'' mechanisms.[8,9] In previous studies on SnO_2 nanowires/nanobelts, the samples were not intentionally doped and the carriers typically originated from oxygen deficiencies.[10–15] Intentional doping of SnO_2 nanowires was reported recently by our group.[16,17] Herein, we report systematic studies of the effect of Sb doping on SnO_2 nanowires and detailed electrical characterization of the nanowire devices. Our results demonstrate that undoped SnO_2 nanowires show Schottky contact to Ti/Au electrodes in air and are suitable for the detection of UV light. Lightly Sb-doped nanowires are promising as high-performance nanowire transistors, and degenerately Sb-doped SnO_2 nanowires are transparent metallic conductors with resistivities as low as $4.09 \times 10^{-4}\ \Omega\,cm$.

Undoped, lightly (<0.5%), and heavily (2–4%) Sb-doped SnO_2 nanowires were grown on Si(100) substrates at 900 °C by a vapor-transport method that employs the vapor–liquid–solid (VLS) growth mode (see Experimental Section). Figure 1a shows a low-magnification transmission electron microscopy (TEM) image of the as-synthesized heavily Sb-doped SnO_2 nanowires. The catalyst nanoparticles are clearly visible on the tips of the nanowires, which confirms the VLS growth mode. High-resolution TEM (HRTEM; Figure 1b) confirms that the SnO_2 nanowires are single crystals with a tetragonal rutile structure, and verifies that the dislocations or amorphous surface layers that are often found in other nanostructures are absent in the SnO_2 nanowires.

Figure 2a shows the current–voltage ($I_{ds} - V_{ds}$; ds = drain–source) characteristics of an undoped SnO_2 nanowire device. A rectifying behavior (curve a) was normally observed in air in the dark, which indicates the formation of Schottky barriers at the metal/semiconductor contact. Upon illumination by UV light (254 nm), a linear current–voltage (ohmic-like) response (curve c) was observed along with a much higher current level. The ohmic-like behavior can be explained by enhanced electron tunneling at the metal/semiconductor interface due to an increase of the carrier density and reduction of the depletion width upon illumination with above-bandgap photons, as reported for ZnO nanowire Schottky diodes.[18,19]

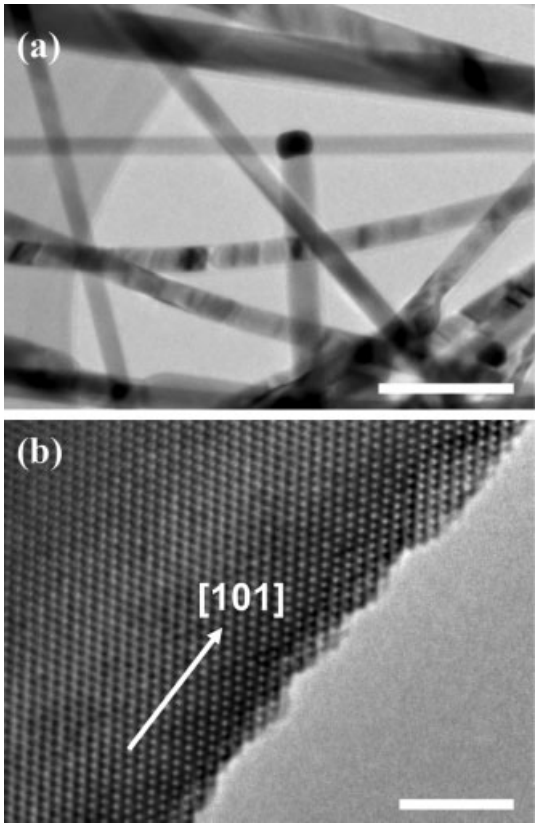

Figure 1. a) Low-magnification TEM image of degenerately Sb-doped SnO_2 nanowires. Scale bar: 100 nm. b) HRTEM image of a single SnO_2 nanowire. Scale bar: 5 nm.

[*] Dr. Q. Wan, E. Dattoli, Prof. Wei Lu
Department of Electrical Engineering and Computer Science
University of Michigan
Ann Arbor, MI 48109 (USA)
Fax: (+734) 763-9324
E-mail: wluee@eecs.umich.edu; wanqing76@hnu.cn
Dr. Q. Wan
Micro-Nano Technologies Research Center
Hunan University
Changsha 410082 (P.R. China)

[**] Q.W. acknowledges support from the National Science Foundation (NSF) of China (grant number 50602014), the Program for New Century Excellent Talents at Hunan University, and the Foundation for the Author of National Excellent Doctoral Dissertation of China (200752). W.L. acknowledges support from the NSF (ECS-0601478) and the Rackham Faculty Research Grant.

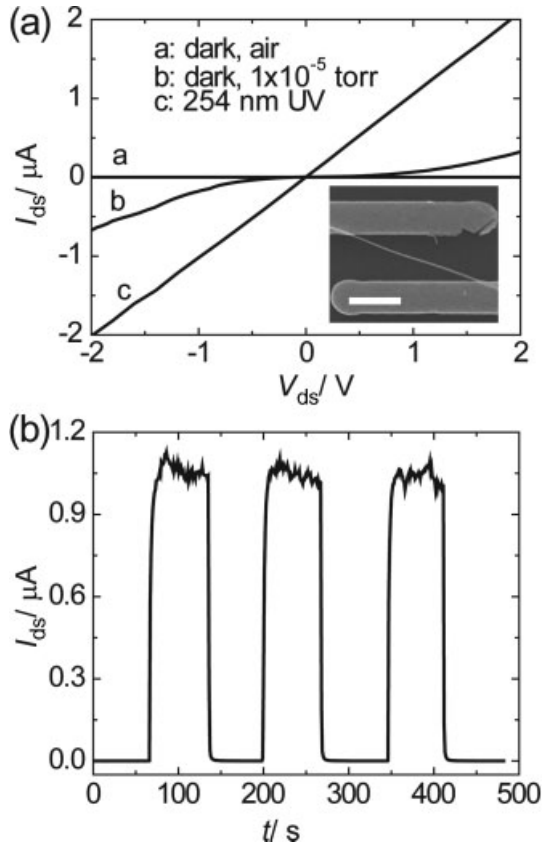

Figure 2. Electrical properties of an undoped SnO_2 nanowire. a) $I_{ds} - V_{ds}$ curves of a nanowire device measured in the dark (curve a, in air and curve b, in vacuum) and exposed to 254-nm UV (curve c, in air). Inset: scanning electron microscopy (SEM) image of the SnO_2 nanowire device. Scale bar: 3 μm. b) Reversible switching of the nanowire device between low- and high-resistivity states as the UV light was turned on and off at different times *t*. The voltage bias on the nanowire was −1 V.

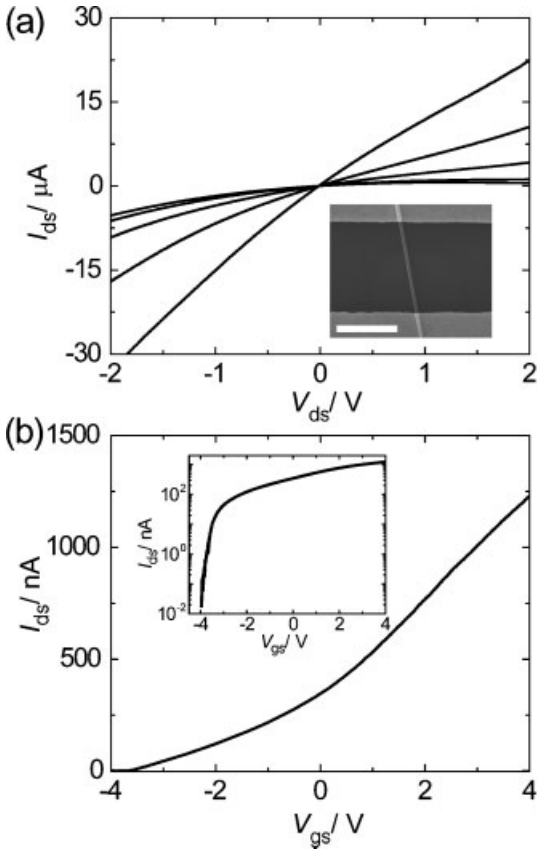

Figure 3. Electrical properties of a lightly Sb-doped SnO_2 nanowire configured as a FET device. a) Family of $I_{ds} - V_{ds}$ curves at different gate–source V_{gs}. V_{gs} was varied from +4 to −4 V in steps of −2 V and the device was measured in air at room temperature. Inset: SEM image of the device. Scale bar: 1.5 μm. b) Transfer ($I_{ds} - V_{gs}$) curve of the same nanowire device at $V_{ds} = 0.1$ V. Inset: semilog plot of the $I_{ds} - V_{gs}$ curve.

In comparison, a smaller increase in current was observed when the sample was measured in a vacuum (10^{-5} Torr) without UV illumination (curve b), where the increase in carrier concentration was attributed to oxygen desorption alone.[14]

Figure 2b shows the response of the device as a function of time (t) as the UV source was switched on and off. The current rapidly increases from 2 pA to 1 μA upon UV illumination, and the device can be reversibly switched between the low- and high-conductance states with the response and recovery times estimated to be ≈1 s. The photocurrent sensitivity was estimated to be $\approx 5 \times 10^5$, a value much higher than that reported for undoped SnO_2 nanowire devices with ohmic contacts,[15] due partly to the small dark current. The responsivity (R_{res}) for the device was estimated to be 6.25×10^6 mA W^{-1}. The photoconductive gain, defined as the ratio of the number of electrons collected per unit time and the number of photons absorbed per unit time, was estimated from the photon flux and the measured photocurrent to be 3000 (see Experimental Section). The high photoconductive gain is comparable to earlier studies on ZnO nanowire photodetectors operating under similar conditions,[20] and is a consequence of the long photocarrier lifetime combined with the short carrier transient time in nanowire devices.[20,21] The fast response time, high photocurrent sensitivity, and responsivity suggest that SnO_2 nanowire Schottky diodes are suitable candidates as UV photodetectors or photoswitches.

The undoped SnO_2 nanowire devices, however, show very poor transistor behavior in air due to their high resistivity and the formation of Schottky contacts. The electrical performance of SnO_2 nanowires can be significantly improved by Sb doping. Figure 3a shows typical $I_{ds} - V_{ds}$ curves at different gate–source (V_{gs}) for a lightly Sb-doped SnO_2 nanowire configured as a field-effect transistor (FET) device. Linear $I_{ds} - V_{ds}$ curves were always observed for Sb-doped SnO_2 nanowire devices at low biases, which indicates low-resistance ohmic contacts between the nanowire channel and the Ti/Au electrodes. $I_{ds} - V_{gs}$ curves obtained for the Sb-doped SnO_2 nanowire FET show that the device operates in the depletion mode as a result of effective n-type doping with a transconductance g_m of 236 nS and an electron

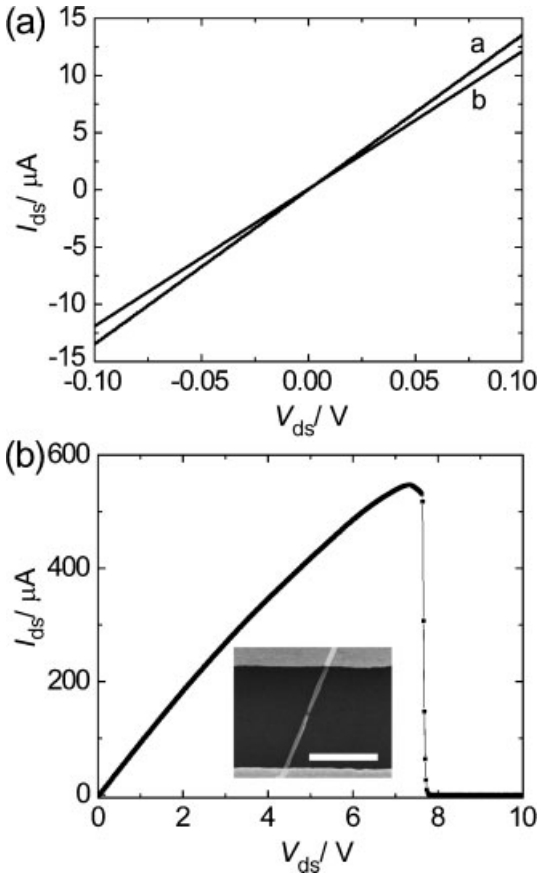

Figure 4. a) $I_{ds} - V_{ds}$ characteristics of a SnO_2:Sb nanowire device measured in air without (curve b) and with (curve a) illumination by 254-nm UV light. b) $I_{ds} - V_{ds}$ curve recorded for the same SnO_2:Sb nanowire device, which shows the breakdown at very high current densities. The SnO_2:Sb nanowire can carry a current of more than 0.5 mA before breaking down. Inset: SEM image of the failed nanowire, which shows that failure occurs in the middle of the nanowire. Scale bar: 1 μm.

mobility of 550 $cm^2\ V^{-1}\ s^{-1}$ at $V_{ds} = 0.1$ V. The on/off ratio and subthreshold slope for the Sb-doped SnO_2 FET device are 1×10^5 and 0.17 V $decade^{-1}$ at $V_{ds} = 0.1$ V, respectively. The excellent electrical properties confirm that the lightly doped SnO_2 nanowires are well-suited for transistor applications, as reported in our recent studies.[17]

The SnO_2 nanowires can be further doped to show metallic behavior by increasing the Sb:Sn ratio in the source during nanowire growth. The electrical properties of a degenerately (2–4 at%) Sb-doped SnO_2 (SnO_2:Sb) nanowire are shown in Figure 4 with an estimated resistivity of $5.8 \times 10^{-4}\ \Omega$ cm in the dark. Due to the much higher carrier concentration, the SnO_2:Sb nanowire shows a much smaller response (about 11.0%) to the same UV light compared to the undoped nanowire. As reported earlier,[16] the SnO_2:Sb nanowires can also endure a high current density before failure. The failure current of 0.572 mA in Figure 4b corresponds to a current density of $1.95 \times 10^7\ A\ cm^{-2}$. The low resistivity and high failure density in turn make the SnO_2:Sb nanowires desirable for applications such as nanoscale interconnects and electron field emitters.

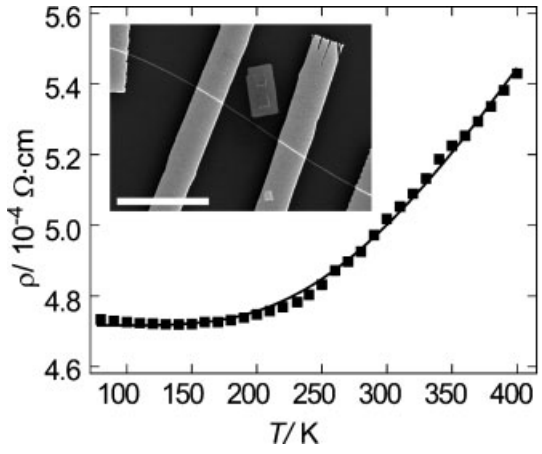

Figure 5. Temperature (T) dependence of the resistivity (ρ) of a SnO_2:Sb nanowire from 77 to 400 K. Inset: SEM image of the device. Scale bar: 10 μm.

The metallic behavior of SnO_2:Sb nanowires was further proved by temperature-dependent resistivity measurements. As shown in Figure 5, a four-probe setup was used to measure the resistivity ρ of a SnO_2:Sb nanowire at various temperatures T from 400 to 77 K inside a cryogenic probe station. The resistivity versus temperature data agree well with the Block–Grüneisen curve (solid line) expected for a metal or degenerately doped semiconductor.[22] At high temperatures, the resistivity increases linearly from 4.9×10^{-4} to 5.4×10^{-4} Ω cm from 273 to 400 K. This behavior is in turn consistent with the linear resistivity–temperature relationship expected for a metal at high temperatures when scattering is dominated by the electron-acoustic phonon scattering mechanism.[23]

In conclusion, we have shown that Sb doping has significant influence on the electrical properties of SnO_2 nanowires. Undoped SnO_2 nanowires are hardly conducting and form Schottky contacts with metal electrodes. The nanowire Schottky devices are suitable in UV photodetector applications. On the other hand, lightly Sb-doped SnO_2 nanowires are well-suited to high-mobility transistor applications. A further increase in the doping level results in degenerately Sb-doped SnO_2 nanowires that show metallic behavior with resistivity as low as $5.8 \times 10^{-4}\ \Omega$ cm and failure-current density as high as $\approx 1.95 \times 10^7\ A\ cm^{-2}$.

Experimental Section

Undoped, lightly, and degenerately Sb-doped SnO_2 nanowires were grown by the VLS process. The source material, high-purity (99.99%) powders of Sn or a Sn:Sb mixture, was first loaded in an alumina boat. Growth substrates of Si(100) covered with a 10-nm-thick Au film were placed on top of the boat. The alumina boat was then positioned at the center of an alumina tube that was inserted into a horizontal tube furnace. The furnace was heated from room temperature to 900 °C at a rate of 20 °C min^{-1} under a flow of Ar (500 sccm) with a trace amount of oxygen. The growth time was 1 h at 900 °C. The furnace was then cooled to

room temperature at a rate of 5 °C min^{-1}. After nanowire growth, morphological investigations were performed by field-emission SEM (XL30FEG). For further structural studies, the nanowires were removed from the Si growth substrate by sonication in isopropyl alcohol and then deposited on carbon-coated copper grids for TEM (JEOL-3011) characterization. To fabricate nanowire devices, the nanowires in isopropyl alcohol solution were deposited onto a degenerately doped n-type silicon substrate capped with a 50-nm silicon dioxide (SiO_2) layer. A photolithography or electron-beam (e-beam) lithography process was then used to define pairs of metal electrodes on the SiO_2/Si substrate, followed by metal deposition of Ti/Au (10/100 nm) by e-beam evaporation to complete the structure of the device. Prior to metal evaporation, the samples were cleaned with an O_2 plasma (50 W) for 30–60 s to remove possible resist residue. The photoresponsivity was estimated from $R_{res} = I_p/(I_{irr} \times A)$, where A is the effective device area, I_p is the photocurrent, and I_{irr} is the irradiance of the incident light. The incident UV light power was 4 W, the irradiance I_{irr} to the nanowire devices was 0.04 W cm^{-2}, and A was 0.4 μm^2. The photocurrent was defined as $I_p = I_{light} - I_{dark} = 1$ μA. The incident radiant energy to the nanowire per second was 1.6×10^{-9} J. The energy of the 254-nm photon was $E_p = 7.8 \times 10^{-19}$ J, which corresponded to a flux of 2.1×10^9 photons per second incident on the nanowire. The measured photocurrent ($I_p = 1$ μA) corresponded to approximately 6.25×10^{12} carriers per second.

Keywords:
conductors · doping · nanowires · photodetectors · transistors

[1] M. Batzill, U. Diebold, *Prog. Surf. Sci.* **2005**, *79*, 47–154.
[2] S. Chakraborty, A. Sen, H. S. Maiti, *Sens. Actuators B* **2006**, *115*, 610–613.
[3] O. Wurzinger, G. Reinhardt, *Sens. Actuators B* **2004**, *103*, 104–110.
[4] H. Kim, A. Piqué, *Appl. Phys. Lett.* **2004**, *84*, 218–220.
[5] S. W. Lee, Y. W. Kim, D. Chen, *Appl. Phys. Lett.* **2001**, *78*, 350–352.
[6] P. I. Archer, P. V. Radovanovic, S. M. Heald, D. R. Gamelin, *J. Am. Chem. Soc.* **2005**, *127*, 14 479–14 487.
[7] S. B. Ogale, R. J. Choudhary, J. P. Buban, S. E. Lofland, S. R. Shinde, S. N. Kale, V. N. Kulkarni, J. Higgins, C. Lanci, J. R. Simpson, N. D. Browning, S. Das Sarma, H. D. Drew, R. L. Greene, T. Venkatesan, *Phys. Rev. Lett.* **2003**, *91*, 077 205.
[8] S. C. Erwin, L. J. Zu, M. I. Haftel, A. L. Efros, T. A. Kennedy, D. J. Norris, *Nature* **2005**, *436*, 91–94.
[9] G. M. Dalpian, J. R. Chelikowsky, *Phys. Rev. Lett.* **2006**, *96*, 226 802.
[10] Z. W. Pan, Z. R. Dai, Z. L. Wang, *Science* **2001**, *291*, 1947–1949.
[11] Z. R. Dai, J. L. Gole, J. D. Stout, Z. L. Wang, *J. Phys. Chem. B* **2002**, *106*, 1274–1279.
[12] Y. Liu, M. Liu, *Adv. Funct. Mater.* **2005**, *15*, 57–62.
[13] B. Cheng, J. M. Russell, W. S. Shi, L. Zhang, E. T. Samulski, *J. Am. Chem. Soc.* **2004**, *126*, 5972–5973.
[14] M. S. Arnold, P. Avouris, Z. W. Pan, Z. L. Wang, *J. Phys. Chem. B* **2003**, *107*, 659–663.
[15] Z. Liu, D. Zhang, S. Han, C. Li, T. Tang, W. Jin, X. Liu, B. Lie, C. W. Zhou, *Adv. Mater.* **2003**, *15*, 1754–1757.
[16] Q. Wan, E. N. Dattoli, W. Lu, *Appl. Phys. Lett.* **2007**, *90*, 222 107.
[17] E. N. Dattoli, Q. Wan, W. Guo, Y. Chen, X. Pan, W. Lu, *Nano Lett.* **2007**, *7*, 2463–2469.
[18] Y. W. Heo, C. Tien, D. P. Norton, S. J. Pearton, B. S. Kang, F. Ren, J. R. LaRoche, *Appl. Phys. Lett.* **2004**, *85*, 3107–3109.
[19] K. Keem, H. Kim, G. T. Kim, J. S. Lee, B. Min, K. Cho, M. Y. Sung, S. Kim, *Appl. Phys. Lett.* **2004**, *84*, 4376–4378.
[20] H. Kind, H. Yan, B. Messer, M. Law, P. D. Yang, *Adv. Mater.* **2002**, *14*, 158–160.
[21] C. Soci, A. Zhang, B. Xiang, S. A. Dayeh, D. P. R. Aplin, J. Park, X. Y. Bao, Y. H. Lo, D. Wang, *Nano Lett.* **2007**, *7*, 1003–1009.
[22] J. M. Ziman, in *Electrons and Phonons*, Clarendon Press, Oxford, UK, **1960**.
[23] N. W. Ashcroft, N. D. Mermin, in *Solid State Physics*, Brooks Cole, New York **1976**.

Received: August 24, 2007
Revised: December 4, 2007
Published online: March 27, 2008

